





## Optical turbulence control by non-Hermitian potentials

Salim B. Ivars <sup>1,\*</sup>, Muriel Botey <sup>1</sup>, Ramon Herrero <sup>1</sup> and Kestutis Staliunas <sup>1,2,3</sup>

<sup>1</sup>*Departament de Física, Universitat Politècnica de Catalunya, Rambla Sant Nebridi 22, Terrassa 08222, Barcelona, Catalonia, Spain*

<sup>2</sup>*Institució Catalana de Recerca i Estudis Avançats, Passeig Lluís Companys 23, Barcelona E-08010, Spain*

<sup>3</sup>*Vilnius University, Faculty of Physics, Laser Research Center, Sauletekio Ave. 10, Vilnius, Lithuania*



(Received 23 March 2021; revised 17 September 2021; accepted 22 February 2022; published 15 March 2022)

We propose a method for a control of turbulence by modifying the excitation cascade leading to turbulence. The method is based on the asymmetric coupling between the spatiotemporal excitation modes by non-Hermitian potentials. The non-Hermitian potentials are recently known to enable unidirectional coupling between modes. We demonstrate that such unidirectional coupling towards larger (smaller) wave numbers can increase (reduce) the energy flow in turbulent states, and therefore, influence the character of turbulence. The study is based on the complex Ginzburg-Landau equation, a universal model for pattern formation and turbulence in a wide range of systems including nonlinear optical resonators. We show that enhancement or reduction of turbulence is indeed dependent on the imposed direction of the energy flow, controlled by the phase shift between the real and imaginary parts of the temporal oscillation of the non-Hermitian potential.

DOI: [10.1103/PhysRevA.105.033510](https://doi.org/10.1103/PhysRevA.105.033510)

### I. INTRODUCTION

In spite of the intensive efforts of the last century to build the dynamical theory of turbulence, pioneered by Landau [1], Kolmogorov [2], Richardson [3], Arnold [4], Lorentz [5], and others, the dynamical mechanisms of turbulence are still not completely understood, remaining as a long-standing problem. Different physical systems show different kinds of turbulence (in the atmosphere [6], in fluids [7], in optics [8], and in financial markets [9]). An attempt at classification may be in terms of weak [10], intermittent [11], and strong turbulence [12] or dynamical chaos [13]. The descriptive (phenomenological) analysis of turbulence, however, goes far back in time, see Reynolds [14], Prandl [15], or even to ancient times.

Despite some confusion in the quantitative understanding of turbulence, a major class of turbulent systems follow quite a general scenario. The general picture is that the excitations imposed on a large spatial scale in a continuous system migrate through spatial scales due to different nonlinear wave-mixing processes, until finally entering into a dissipative wavelength range on a small spatial scale. This results in an energy cascade through the spatial scales, or equivalently, through wave numbers, where turbulence bridges the input and output scales. Most celebrated is the excitation energy distribution of Kolmogorov  $E(k) \sim k^{-5/3}$  in the inertial range [16], i.e., between the large scale of imposed excitation ( $k_{\text{exc}} \sim 1/d_{\text{exc}}$  is small) and the small space scale where viscosity dominates ( $k_{\text{dis}} \sim 1/d_{\text{dis}}$  is large). Although the Kolmogorov  $-5/3$  law is strictly valid for three-dimensional (3D), isotropic, homogeneous systems, qualitatively the idea of the excitation cascade through wave numbers is applicable to a wide range of systems [for instance, in two-dimensional

(2D) case, turbulence follows a power law with different power factor, inverse cascade appears, etc.].

### II. MODEL

We here propose a mechanism to influence this excitation cascade through spatial scales, with the purpose to affect the turbulence. Turbulence is simulated by probably one of the simplest and most universal mathematical models, the Complex Ginzburg-Landau Equation (CGLE). CGLE models a wide range of physical systems covering from nonlinear waves to second-order phase transitions, from superconductivity, superfluidity, and Bose-Einstein condensation to liquid crystals and strings in field theory [17]. As written in one of several possible conventions, it reads

$$\frac{\partial A}{\partial t} = (1 + i\alpha)A(1 - |A|^2) + (d - i)\nabla^2 A + iV(\mathbf{r}, t)A, \quad (1)$$

where, the order parameter  $A(\mathbf{r}, t)$  is a complex function of time  $t$  and space  $\mathbf{r}$  [we analyze one-dimensional (1D) and 2D cases],  $\alpha$  is the self-focusing coefficient,  $d$  the diffusion coefficient, and  $V(\mathbf{r}, t)$  is a complex valued potential. The gain and dispersion coefficients are normalized to unity, without loss of generality. For  $\alpha > d$  the homogeneous solution of Eq. (1) is unstable, and the Modulational Instability (MI) of the homogeneous solution induces low-scale perturbation into the system.

The CGLE was systematically derived as an order parameter equation for a variety of continuous systems, hydrodynamical [18–20], chemical [21,22], or optical [23–25], in different orders of approximation. The CGLE can be derived from general symmetry considerations as well: it is the normal form (the minimum equation) describing the lowest-order phase-invariant nonlinearity (the cubic one), space isotropy (Laplacian), gain, dissipation, and MI. Note that, in

\*Corresponding author: [salim.benadouda@upc.edu](mailto:salim.benadouda@upc.edu)

a conservative limit, the CGLE converts into the nonlinear Schrödinger equation describing the quantum hydrodynamics. The CGLE shows different turbulent regimes [26]. Also some approaches were done to control these different turbulent regimes by means of the introduction of delayed global feedback [27–29], local injections [30,31], or introducing localized inhomogeneities [29,32]. In optics, multitransverse mode lasers are also governed by a two-dimensional CGLE in the lowest-order approximation. Energy is injected on large spatial scales (the pump is usually relatively homogeneous), which primarily feeds the lowest-order transverse modes of the laser cavity. Nonlinear processes (four-wave mixing) cause the energy transfer from lower- to higher-order modes. Finally, the highest-order transverse modes are dissipated due to intrinsic diffusion, and also due to the aperture effects included in the potential,  $V(\mathbf{r}, t)$ . This excites a turbulent state with a flow of energy through the transverse modes, which leads to a particular statistical distribution of the transverse modes' excitation. Optical turbulence involves an intricate intermode coupling, a combination of a linear part given by background potential  $V(\mathbf{r}, t)$  (accounting for the gain and refraction index profile in the optical case) and a nonlinear mode coupling due to the intrinsic nonlinearity of the system. In the usual case of Hermitian potentials, the linear part of the mode coupling is bidirectional and symmetric. For instance, for the 1D simple real-valued potential  $V(\mathbf{r}) \sim \cos(qx) = [\exp(iqx) + \exp(-iqx)]/2$  the spatial modulation with wave numbers  $\pm q$  symmetrically couples any mode  $k$  with modes  $k + q$  and  $k - q$ .

Recently, it was discovered that non-Hermitian potentials can induce asymmetric or even unidirectional coupling between the modes. In particular, such a situation occurs for the so-called Parity-Time (PT) symmetric systems close to the phase transition point [33–35]. For potentials with complex-valued amplitudes of the modulation (involving gain or loss and refractive index modulations in the case of optics) constructed in the form  $V(\mathbf{r}) \sim \cos(qx) + i \sin(qx) = \exp(iqx)$ , the mode coupling becomes, evidently, unidirectional: the mode  $k$  is efficiently coupled to mode  $k + q$  by such a potential, but not vice versa, as the  $\exp(-iqx)$  component in the potential  $V(\mathbf{r})$  is absent.

The idea prompted by this article is to make use of the asymmetric mode coupling to influence the excitation cascade of optical turbulence by dominantly coupling modes towards modes with either smaller or larger wave vectors (modulus). In other words, we aim to control turbulence by introducing a unidirectional coupling towards either lower- or higher-order transverse modes. However, such a spatially unidirectional coupling potential alone would not solve our intentions to influence the energy cascade through spatial scales. While a modulation component with a positive wave number  $q$  would couple modes with negative wave numbers to lower-order modes (with a wave-number modulus closer to zero values  $-|k| + q$ ), it would, in turn, couple the waves with positive wave numbers towards higher-order modes (with the wave-number modulus further away from zero,  $|k| + q$ ). Therefore, while breaking the symmetry in the wave-number domain, this does not affect the energy cascade throughout the spatial scales, neither towards larger nor towards smaller wave numbers. We propose to solve this

issue by introducing asymmetric mode coupling in the frequency domain. The different modes in Eq. (1) oscillate with different frequencies and the traveling wave solution  $A(\mathbf{r}, t) = (1 - dk^2)^{1/2} \exp(i\mathbf{k}\mathbf{r} + i\omega t)$  obeys the parabolic dispersion relation  $\omega(k) = k^2$ . Generally, in turbulence a continuum of excitations appear, therefore the dispersion plays an indicative role only. To explore the turbulence spectra we numerically integrate the 1D CGLE, using a conventional split-step method, and calculate the Fourier spectrum of the recorded solution, both in space and in time. A snapshot of the turbulent field is displayed in Fig. 1(a). Its spectrum is merely a cloud of points in  $(k, \omega)$  space, indeed distributed around the dispersion parabola, see Fig. 1(b).

Next, we want to introduce a potential that induces asymmetry in the coupling to higher- or lower-order modes. A spatiotemporally modulated Hermitian potential  $V(\mathbf{r}, t) = \cos(qx) \cos(\Omega t) = 1/4 \sum_{\pm} \exp(\pm iqx \pm i\Omega t)$  would couple a particular mode  $(k, \omega)$  to four modes  $(k \pm q, \omega \pm \Omega)$  as indicated by the arrows in Fig. 1(b). Evidently, the coupling components indicated by arrows 1 and 4 do not result in a functional coupling since they couple the resonant modes to the nonresonant ones (located further away from the dispersion curve in double Fourier space). The other coupling components indicated by arrows 2 and 3 couple to the higher- and lower-frequency (and wave number) modes, respectively. Therefore, such spatiotemporal modulation of the potential does not lead to a unidirectional mode coupling to low (high) order modes.

The coupling asymmetry between low- and high-order modes can be imposed by the non-Hermitian character of the temporal part of the modulation of the potential:  $V(\mathbf{r}, t) = \cos(qx) \exp(-i\Omega t) = 1/2 \sum_{\pm} \exp(\pm iqx - i\Omega t)$ . Such a coupling from  $(k, \omega)$  excites the modes with  $(k \pm q, \omega - \Omega)$ , i.e., only the coupling arrows 1 and 2 are present in the diagram. Having in mind that the coupling arrow labeled as 1 is nonfunctional  $(k, \omega) \rightarrow (k + q, \omega - \Omega)$  maintains the functional coupling  $(k, \omega) \rightarrow (k - q, \omega - \Omega)$ , corresponding to arrow 2 in Fig. 1. This introduces a unidirectional coupling towards lower frequency and smaller  $|k|$  modes. Analogously, the modulation of the potential  $V(\mathbf{r}, t) = \cos(qx) \exp(+i\Omega t)$  would result in functional coupling indicated by arrow 3, i.e., towards higher frequencies and larger wave numbers. Both situations are, respectively, depicted in Figs. 1(c) and 1(d), where the 1D turbulent system is modulated with the above-proposed non-Hermitian spatiotemporal potentials. Temporal modulation with  $-\Omega$  favors an efficient coupling towards lower-order modes (indicated by arrows), and the energy cascade accumulates the spectrum intensity near  $k = 0$  [Fig. 1(c)]. In contrast,  $\Omega$  favors the energy cascade towards higher-order modes, thus supporting the energy flow towards higher wave numbers  $|k|$  and enhancing the turbulence [Fig. 1(d)].

This is the physical idea of the article. Next follows the numerical verification of the proposal. By integrating the CGLE numerically and manipulating the shapes of the complex potential, we indeed manage to influence the turbulence cascade. We show, in particular, that the width of the spectrum of excited spatial modes depends on the phase-shift between the real and imaginary parts of the temporal modulation of the potential.

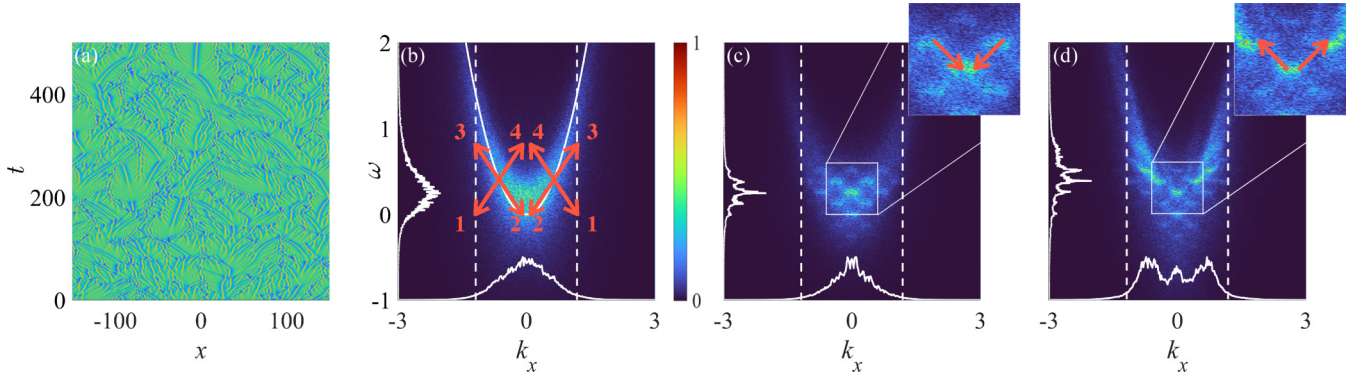


FIG. 1. Turbulence spectra. (a) Temporal evolution of the intensity of the turbulent field. (b) Intensity of the spatiotemporal Fourier spectrum  $|A(k_x, \omega)|^2$  of a 1D turbulent system. Dashed lines show the unstable spatial modes range. Solid lines correspond to integrals of the spectrum intensity over  $\omega$  and  $k_x$ , respectively. The parabola in (a) represents the parabolic dispersion  $\omega = k_x^2$ . (c) and (d) show spectral intensity of the system with an inward and outward non-Hermitian coupling. The arrows in (b) indicate all possible mode couplings, while in (c) and (d) correspond to the efficient unidirectional mode couplings. (b), (c), and (d) share same color map.  $\alpha = 0.7$  and  $d = 0.03$  for all three figures.

### III. RESULTS

Note that, while discussing the general CGLE, we refer to the optical system since, in optics, in laser-like systems, it is relatively easy to manipulate the real and imaginary parts of the potential (gain and refractive index, respectively), contrary to other systems described by the CGLE. To be concise, we introduce the spatiotemporally modulated potential

$$V(\mathbf{r}, t) = V(\mathbf{r})[m_1 \cos(\Omega t) + im_2 \cos(\Omega t + \phi_t)], \quad (2)$$

where  $V(\mathbf{r})$  is the spatial part of the modulation,  $\Omega$  is the temporal modulation frequency,  $m_1$  and  $m_2$  are the amplitudes of the real and imaginary parts of the time modulation, and  $\phi_t$  is the phase shift between them. We assume the resonant case  $\Omega = q^2$ , yet some slight deviation of this condition is also possible due to the spectral fuzziness of the dispersion curve, as explained in detail in the Appendix.

The character of turbulence may be characterized by the second-order moment  $\mu$  of the spatiotemporal Fourier spectrum, which represents the overall width of the turbulent spectrum.

For the 1D case, for  $V(\mathbf{r}) = \cos(qx)$  we analyze the width of the turbulence spectra  $\mu$  in parameter spaces. Figure 2(a) shows the map  $\mu(m_2, \phi_t)$  for equal amplitudes of the real and imaginary parts of the temporal modulation,  $m_1 = m_2$ , exploring the influence of the phase shift between two modulation components. The optimum phase shift that allows the maximally asymmetric coupling between modes  $\phi_{\text{opt}}$  is found to be centered around 0 or  $\pi$ . Note that the maximum asymmetry effect in the conventional theory of stationary PT-symmetric systems occurs at  $\pm\pi/2$  [33]. This apparent inconsistency occurs due to the fact that, in this case, the potential is modulated in time; this point is further discussed in detail below. Figure 2(b) shows a map  $\mu(m_2, m_1)$  for the optimum value of the phase  $\phi_t$ . Interestingly, the optimal ratio of the modulation quadratures  $m_1/m_2$  is proportional to the nonlinearity coefficient  $\alpha$ . We check this conclusion by repeating calculations with different coefficient  $\alpha$ . Figure 2(c) shows the integral spatial spectrum, i.e., the spectrum intensity integrated over time, or equivalently, over the frequency

$I(k) = \int |A(k, \omega)|^2 d\omega$ . It is evident that the coupling towards the higher (lower) order modes broadens (narrows) the integral spectrum  $I(k)$ . However, apart from a global narrowing of the overall spectrum, the spectral distribution becomes more “coherent,” i.e., consisting of discrete modes on a weak turbulent background, see Fig. 2(c) in the case of coupling towards lower modes. The presence of many distinct harmonics on a relatively weak turbulent background is not related to the

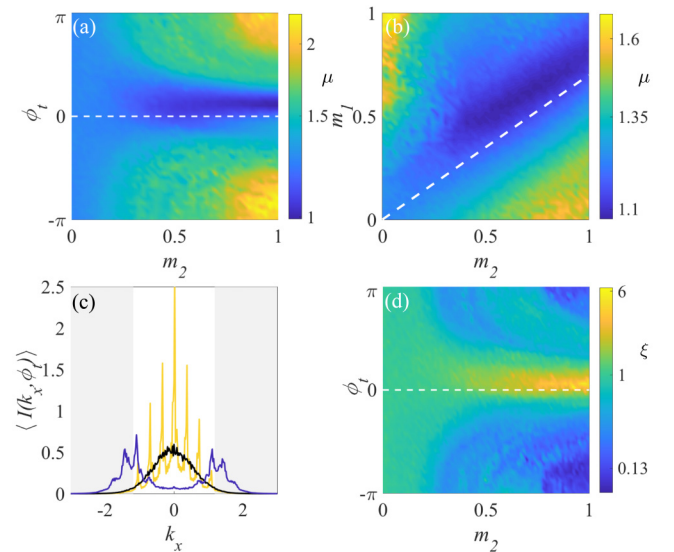


FIG. 2. Taming the turbulent spectrum. (a)  $(m_2, \phi_t)$  map of the overall width of turbulence spectrum,  $\mu$ , with  $m_2 = m_1$ . The white dashed line indicates  $\phi_t = \pi/2 - \arctan(1/\Omega)$ . (b)  $(m_2, m_1)$  map of the second-order momentum  $\mu$ . The white dashed line indicates the slope  $m_1 = \alpha/\sqrt{(\Omega^2 + 1)}m_2$ . (c) Spectra of the unmodulated (black) and modulated CGLE for an inwards coupling (yellow) [ $\phi_t = 0.063$ ,  $m_2 = 0.926$ , and  $m_1 = \alpha m_2$ ] and outwards coupling (lilac) [ $\phi_t = -3.078$ ,  $m_2 = 0.926$ , and  $m_1 = \alpha m_2$ ]. The shaded gray areas indicate the stable modes of the homogeneous solution. (d)  $(m_1, \phi_t)$  map of the normalized central intensity.  $\alpha = 0.7$ ,  $d = 0.03$ ,  $q = 0.356$ , and  $\Omega = q^2$  for all four figures.



additional disorder in the system. Therefore, a better characterization of the strength of the turbulence may be provided by a normalized central intensity of the integral spectrum  $\xi = I(0)/\int_{-\infty}^{\infty} I(k)dk$ , which indicates the level of the condensation of energy into lowest-order modes (homogeneous state), and does not take into account the presence of the coherently excited comb of harmonics. The map of  $\xi$ , shown in Fig. 2(d) evidences the best (worst) condensation to the homogeneous state for the phase difference 0 ( $\pi$ ) between the potential modulation quadratures and it is a good correspondence with Fig. 2(a). In this particular case, the condensation level of  $\xi$  increases by more than one order of magnitude while varying the phase to favor the excitation cascade towards lower (higher) wave numbers. Figure 2(c) shows the integral spectrum, which evidences that, for the modulation favoring an outwards excitation flow ( $\phi_t = \phi_{\text{opt}} - \pi$ ), the energy cascade is directed to high-order modes, yet for the modulation with ( $\phi_t = \phi_{\text{opt}}$ ) the effect is reversed.

The management of the turbulence spectrum can be directly generalized to higher-dimensional systems, for instance, to the 2D one. Figure 3 shows the results of integration of the 2D CGLE for different geometries of the spatial modulation of the potential:  $V(\mathbf{r}) = 1/n \sum_{i=1}^n \cos(\mathbf{q}_i \mathbf{r})$  being the  $\mathbf{q}_i$  lattice vectors. Figures 3(a) and 3(b) provide the unaffected turbulent field and its spectrum while Figures 3(c) and 3(d) correspond to a striped spatial modulation of the potential. The narrowing (broadening) of the turbulent spectrum is evident along the modulated horizontal  $x$  direction, whereas the spectrum along the vertical  $y$  direction remains unaffected. Figures 3(e) and 3(f) show the results for 2D modulation with a square symmetry of the potential. For this potential, the broadening or narrowing of the spectrum occurs in both directions  $k_x$  and  $k_y$ . A similar result is found for a hexagonal modulation (not shown in the article) and for an octagonal modulation depicted in Figs. 3(g) and 3(h).

#### IV. DISCUSSION

This qualitative behavior in 2D systems is analogous to the 1D case, and the narrowing (broadening) of the integral spectrum occurs for the phase shift close to 0 ( $\pi$ ) between the potential modulation quadratures. Some comments are appropriate to interpret the optimum values of the phase shift. A stationary spatial modulation of the potential results in the corresponding modulation of the wave function, in the lowest-order (Born) approximation. For instance, for the potential weakly modulated only in space,  $V(x) = \cos(qx)$ ,

$$A(x) \approx 1 + V(x)(2 + iq^2)/[iq^2(2\alpha - q^2)], \quad (3)$$

as straightly follows from the CGLE (1) in a weak modulation limit  $m \ll 1$ . In other words, the response equally follows both modulation quadratures of the potential, real, and imaginary. Yet, for the temporally modulated potentials, there is a phase shift between the temporal modulation of the potential and the response, which depends on the modulations of the real and imaginaries part of the potential. To achieve the maximal asymmetry of response, the modulation components must be shifted by  $\pm\pi/2$ , however, with a correction:  $\phi_t = \phi' - \arctan(\frac{1}{\Omega})$ , where  $\phi'$  corresponds to the phase shift

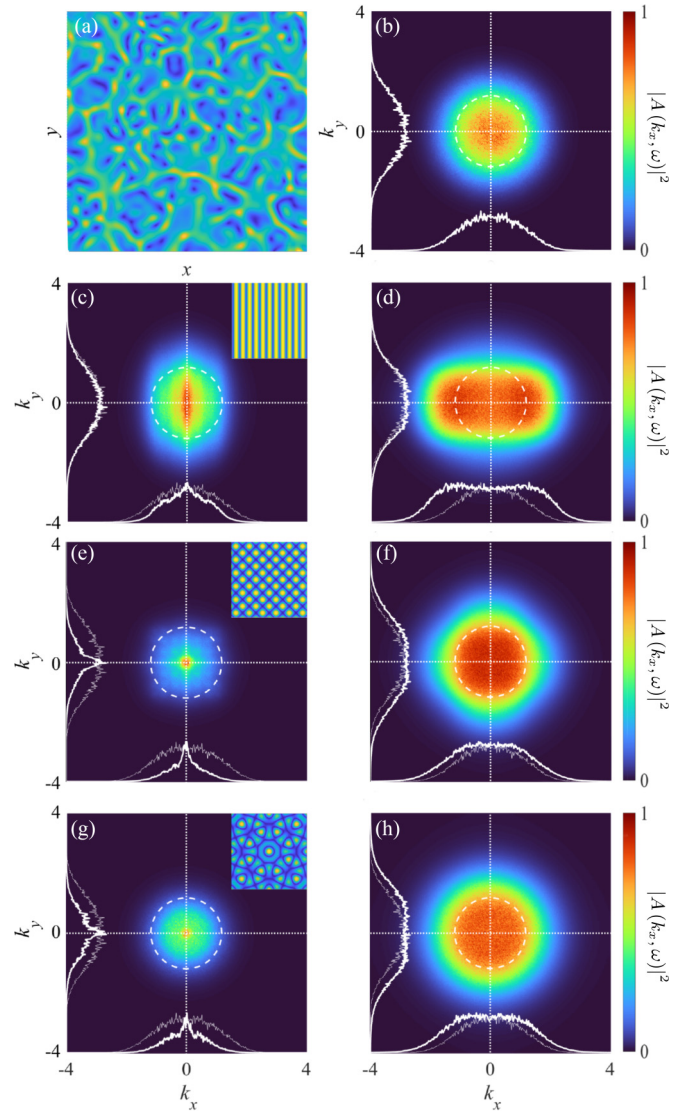


FIG. 3. 2D turbulence. (a) Snapshot of the computed spatial distribution in two space dimensions. (b) Time-averaged turbulent Fourier spectrum intensity for the 2D CGLE. Lattice vectors correspond  $\mathbf{q}_1 = q[1, 0]$ , for (c) and (d),  $\mathbf{q}_1, \mathbf{q}_2 = q[0, 1]$  (e) and (f) and  $\mathbf{q}_1, \mathbf{q}_2, \mathbf{q}_3 = q[\sqrt{2}/2, \sqrt{2}/2], \mathbf{q}_4 = q[\sqrt{2}/2, -\sqrt{2}/2]$  for (g) and (h). Left column corresponds to the a temporal phase shift  $\phi_t = \phi_{\text{opt}}$ , while the right one to  $\phi_t = \phi_{\text{opt}} - \pi$ . The dashed white circle corresponds to the range of unstable spatial modes. Solid white curves correspond to cross sections at  $k_x = 0$  and  $k_y = 0$ . Thin white curves correspond to cross sections at  $k_x = 0$  and  $k_y = 0$  of the unmodulated system.  $\alpha = 0.7$ ,  $d = 0.03$ ,  $q = 0.356$ , and  $\Omega = q^2$  for all four configurations.

without temporal modulation. This issue is mathematically elaborated on the Appendix.

#### V. CONCLUSION

Summarizing, we showed that periodic potentials in space with non-Hermitian modulations in time can significantly influence the excitation cascade mechanism in turbulence. Such potentials may favor the coupling towards lower frequencies and smaller wave numbers, reduce the cascade to turbulence,

and regularize the spatiotemporal spectra. In contrast, potentials that favor coupling towards higher frequencies and larger wave numbers enhance the turbulence cascade, broadening the turbulence spectra. The proposed turbulence control mechanism is mainly governed by the phase shift between the real and imaginary parts of the complex temporal modulation and their amplitude ratio. We prove this general idea on the CGLE for 1D and 2D systems with different spatial modulation arrangements: linear, square grid, hexagonal, and octagonal. The proposed turbulence control method could be, in principle, implemented in different physical systems for being proved in a universal model. Most promisingly, this method can be particularly useful for controlling turbulence in nonlinear optics in models based on the CGLE, such as broad area lasers and nonlinear resonators.

### ACKNOWLEDGMENTS

This work received funding from the European Social Fund (Project No. 09.3.3- LMT-K712-17- 0016) under a grant agreement with the Research Council of Lithuania (LMTLT), from the Spanish Ministerio de Ciencia e Innovación under Grant No. 385 (PID2019-109175GB-C21).

### APPENDIX A: OPTIMUM PHASE SHIFT BETWEEN TEMPORAL MODULATION QUADRATURES

For the analytical treatment it is more convenient to rewrite the potential [Eq. (2)] in the following form:

$$V(x, t) = \cos(qx)[(m_1 + im_2 e^{i\phi_t})e^{i\Omega t} + (m_1 + im_2 e^{-i\phi_t})e^{-i\Omega t}]. \quad (\text{A1})$$

A nonzero homogeneous solution of the unmodulated CGLE  $A_0 = 1$  is subjected to a small perturbation  $a$ :  $A = A_0 + a$ . Linearization of  $A$  in the CGLE and around  $A_0$  leads to  $\partial_t a = -(1 + i\alpha)(a + a^*) + (d - i)\nabla^2 a + iV(x, t)$ . The perturbation  $a$  corresponds to the driven Bogoliubov mode of CGLE, and consists of the positive and negative frequency components  $a = \cos(qx)[a_+ \exp(i\Omega t) + a_- \exp(-i\Omega t)]$ . In the presence of the modulation of potential the Bogoliubov modes are driven by the potential and can enter into the stationary regimes. Neglecting the small diffusion in the CGLE, we obtain

$$\begin{aligned} i\Omega a_+ &= -(1 + i\alpha)(a_+ + a_-^*) + iq^2 a_+ + im_1 - m_2 e^{i\phi_t}, \\ -i\Omega a_- &= -(1 + i\alpha)(a_+^* + a_-) + iq^2 a_- + im_1 - m_2 e^{-i\phi_t}, \end{aligned} \quad (\text{A2})$$

which can be explicitly solved, for instance, with respect to  $a_+$ :

$$a_+ = \frac{m_1(\Omega + q^2 - 2i) + im_2 e^{i\phi_t}(\Omega + q^2 - 2\alpha)}{\Omega(\Omega - 2i) + q^2(2\alpha - q^2)}. \quad (\text{A3})$$

The amplitude of the excited Bogoliubov mode  $|a_+|$  depends on the phase shift of the temporal part of the potential  $\phi_t$ , as follows from Eq. (A3). Considering the resonant case  $\Omega = q^2$  (the general case leads to more clumsy expressions but does not affect the main conclusion), the expression (A3) simplifies to

$$a_+ = \frac{m_1 \sqrt{\Omega^2 + 1} e^{-i\phi'} + im_2(\Omega - \alpha)}{\Omega(\alpha - i)} e^{i\phi_t}, \quad (\text{A4})$$

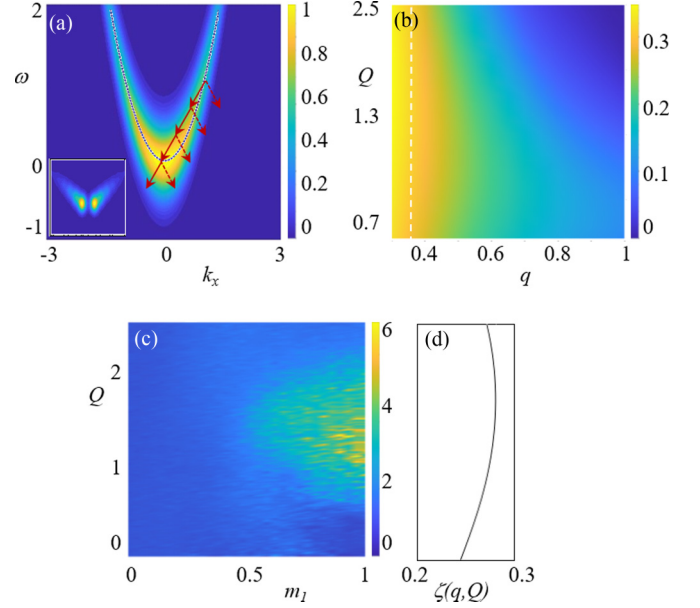


FIG. 4. (a) Phenomenological intensity spectrum distribution  $|A(k, \omega)|^2$ . The inset corresponds to the mode coupling probability  $C(k, \omega)$ . (b) Total energy transfer  $\zeta(q, Q)$ . (c) Integral spectrum  $\xi$  mapped as a function of the resonant parameter  $Q$  and the spatial frequency modulation  $q$  for a fixed  $m_1 = m_2 = 0.5$ . We consider a 1D system with a temporal modulation phase shift  $\phi_t = \phi_{\text{opt}}$ . (d) Cross section of (b)  $\zeta(0.356, Q)$ .

containing the modified phase

$$\phi' = \phi_t + \arctan\left(\frac{1}{\Omega}\right). \quad (\text{A5})$$

In the limit  $\Omega \gg 1$  the amplitude of the excited Bogoliubov mode  $|a_+|$  becomes maximal (minimal) for  $\phi_t = \pm\pi/2$ . This is consistent with the general understanding of PT-symmetric systems, stating that the maximally asymmetric coupling occurs for  $\phi_t = \pm\pi/2$  phase shifts between the quadratures of potential modulation. However, for  $\Omega \approx 1$  and especially for  $\Omega \ll 1$  the optimum phase difference shifts towards  $0/\pi$  for minimum or maximum  $|a_+|^2$ . For instance, when  $\phi_t \rightarrow 0$ , the  $|a_+|$  reaches minimum, which implies the maximum coupling “inwards”, i.e., towards the lower-order modes. The minimum values of  $|a_+|$  (at optimum phase shift) are given by

$$|a_+|^2 = \frac{(m_1 \sqrt{\Omega^2 + 1} - m_2 \alpha)^2}{\Omega^2(\alpha^2 + 1)}, \quad (\text{A6})$$

from where we get the relation  $m_2 \alpha = m_1 \sqrt{\Omega^2 + 1}$  to achieve  $|a_+| = 0$ . This is the optimum ratio between the quadratures of the potential modulation.

### APPENDIX B: ROLE OF NONRESONANT TEMPORAL MODULATION

To inspect the role of the temporal potential we define the resonance parameter  $Q = \Omega/q^2$ ,  $\Omega$  the temporal modulation frequency of the non-Hermitian potential and  $q$  the spatial wave number. In the main text we consider the resonant condition  $\Omega = q^2$  that corresponds to  $Q = 1$ . However, by

building the map shown in Fig. 4(c) we observe that this condition is not sharp since, for a sufficiently strong modulation, the range of efficient values of  $Q$  exhibits a certain spread centered around  $Q \approx 1$ . Therefore, we scanned the temporal modulation frequency  $\Omega$  for a fixed value of the spatial modulation  $q$  to explore the spread. It is possible to determine how the resonant condition becomes a more lax condition by considering an initial intensity spectrum distribution  $|A(k, \omega)|^2$ , as shown in Fig. 4(a); which is analogous to the turbulence spectrum from Fig. 2(b). We now assess the probability to transfer energy from each spectral point to the central neighboring mode by all possible successive cascade couplings  $(k, \omega) - n(\pm q, \Omega)$  [marked as red arrows in Fig. 4(a)]. The coupling probability may be evaluated as

$$C(k, \omega) = \sum_n 2^{-n} \exp[-d_n^2(k, \omega)], \quad (\text{B1})$$

where  $d_n^2(k, \omega) = (k \pm nq)^2 + (\omega - n\Omega)^2$  [see inset in Fig. 4(a)] stands for the squared distance between a coupled mode and the central order mode (0,0). We find the total energy transferred to central modes proportional to  $\zeta(q, Q) = \int_{-\infty}^{\infty} |A(k, \omega)|^2 C(k, \omega) d\omega dk$ , see Fig. 4(b). The value of  $Q$  corresponding to the maximal coupling strongly depends on the spatial modulation  $q$ . For large  $q$  values, only  $n = 1$  or small  $n$  couplings contribute to the energy transfer and the maximum is near the resonant condition  $Q = 1$ . However, for small  $q$  values the cascade to reach the central mode involves more steps, yet the optimum relation  $\Omega/q^2$  proportionally increases. In particular, for  $q = 0.356$ , the energy transfer and the function  $\zeta(q, Q)$  exhibit a maximum near  $Q = 1.5$ . Such a maximum is analogous to the maximum obtained in the main text for the integral spectrum  $\xi$  as it is represented in Fig. 4(c).

- 
- [1] L. D. Landau, Dokl. Akad. Nauk USSR **44**, 311 (1944).  
 [2] A. N. Kolmogorov, Cr Acad. Sci. URSS **30**, 301 (1941).  
 [3] L. F. Richardson, *Weather Prediction by Numerical Process* (Cambridge University Press, Cambridge, England, 2007).  
 [4] A. Sommerfeld, *Ein Beitrag zur hydrodynamischen Erklarung der turbulenten fluessigkeitsbewegungen* (Accademia dei Lincei, Rome, 1909).  
 [5] E. N. Lorenz, J. Atmos. Sci. **20**, 130 (1963).  
 [6] P. O. Fanger, A. K. Melikov, H. Hanzawa, and J. Ring, Energy Buildings **12**, 21 (1988).  
 [7] G. Falkovich, K. Gawdzki, and M. Vergassola, Rev. Mod. Phys. **73**, 913 (2001).  
 [8] K. Ikeda, H. Daido, and O. Akimoto, Phys. Rev. Lett. **45**, 709 (1980).  
 [9] M. Kritzman and Y. Li, Financ. Anal. J. **66**, 30 (2010).  
 [10] P. Manneville, in *Chaos—The Interplay Between Stochastic and Deterministic Behaviour* (Springer, New York, 1995), pp. 257–272.  
 [11] B. B. Mandelbrot, J. Fluid Mech. **62**, 331 (1974).  
 [12] M. V. Goldman, Rev. Mod. Phys. **56**, 709 (1984).  
 [13] B. V. Chirikov and D. L. Shepelyansky, Physica D **13**, 395 (1984).  
 [14] O. Reynolds, Philos. Trans. R. Soc. London **186**, 123 (1895).  
 [15] L. Prandtl, Phys. Z. **11**, 1072 (1910).  
 [16] A. N. Kolmogorov, Proc. Roy. Soc. London Ser. A **434**, 15 (1991).  
 [17] I. S. Aranson and L. Kramer, Rev. Mod. Phys. **74**, 99 (2002).  
 [18] C. R. Doering, J. D. Gibbon, D. D. Holm, and B. Nicolaenko, Nonlinearity **1**, 279 (1988).  
 [19] A. Mielke, in *Handbook of Dynamical Systems* (Elsevier, Amsterdam, 2002), Vol. 2, pp. 759–834.  
 [20] P. Le Gal, J.-F. Ravoux, E. Floriani, and T. D. De Wit, Physica D **174**, 114 (2003).  
 [21] M. Ipsen, F. Hynne, and P. G. Sørensen, Int. J. Bifurcation Chaos **7**, 1539 (1997).  
 [22] J. L. Lopez, Stud. Appl. Math. **148**, 248 (2022).  
 [23] K. Staliunas, Phys. Rev. A **48**, 1573 (1993).  
 [24] O. Tasbozan, A. Kurt, and A. Tozar, Appl. Phys. B **125**, 1 (2019).  
 [25] M. Inc, A. I. Aliyu, A. Yusuf, and D. Baleanu, Optik **158**, 368 (2018).  
 [26] P. Manneville, *Instabilities, Chaos and Turbulence*, Vol. 1, (World Scientific, Singapore, 2010).  
 [27] D. Battogtokh and A. Mikhailov, Physica D **90**, 84 (1996).  
 [28] A. C. Casal and J. I. Diaz, in *Recent Trends in Chaotic, Nonlinear and Complex Dynamics* (World Scientific, Singapore, 2022), pp. 455–513.  
 [29] J. B. G. Tafo, L. Nana, C. B. Tabi, and T. C. Kofane, *Research Advances in Chaos Theory* (IntechOpen, London, 2020).  
 [30] J. Xiao, G. Hu, J. Yang, and J. Gao, Phys. Rev. Lett. **81**, 5552 (1998).  
 [31] H. Zhang, B. Hu, G. Hu, Q. Ouyang, and J. Kurths, Phys. Rev. E **66**, 046303 (2002).  
 [32] M. Jiang, X. Wang, Q. Ouyang, and H. Zhang, Phys. Rev. E **69**, 056202 (2004).  
 [33] C. M. Bender and S. Boettcher, Phys. Rev. Lett. **80**, 5243 (1998).  
 [34] W. W. Ahmed, R. Herrero, M. Botey, Y. Wu, and K. Staliunas, Opt. Lett. **44**, 3948 (2019).  
 [35] W. W. Ahmed, R. Herrero, M. Botey, Z. Hayran, H. Kurt, and K. Staliunas, Phys. Rev. A **97**, 033824 (2018).